Novel Hybrid Porous 3D Networks of Lead(II) Diphosphonate and Triphosphonate Containing 1,3,5-Benzenetricarboxylate

Jun-Ling Song,[a] Jiang-Gao Mao,*[a] Yan-Qiong Sun,[a] and Abraham Clearfield[b]

Keywords: Synthetic methods / Lead / Carboxylate ligands / P ligands

Hydrothermal reactions of lead(II) acetate with 1,3,5-benzenetricarboxylic acid (H_3BTC) and a new aminodiphosphonic acid, [3-pyridyl-$CH_2N(CH_2PO_3H_2)_2$] (H_4L^1), or a new aminotriphosphonic acid, [1-{$(H_2O_3PCH_2)_2NCH_2CH_2$-}-piperazine-4-$CH_2PO_3H_2$] (H_6L^2), afforded two novel porous carboxylate–phosphonate hybrids, $[Pb_4(BTC)(HBTC)(HL^1)]\cdot 3H_2O$ (**1**) and $[Pb_6(BTC)_2(HBTC)(H_2L^2)]\cdot 4.5H_2O$ (**2**). The structure of **1** is built from a 3D porous network of lead(II) tricarboxylate and 1D double chains of lead(II) aminodiphosphonate. The structure of **2** contains <002> lead(II) carboxylate–phosphonate hybrid layers, which are cross-linked by 1D double chains of lead(II) phosphonate through the organic groups of both types of ligands, resulting in the formation of a complex 3D porous network. The lattice water molecules in both compounds are located at the micropores of the structures.

Introduction

Open-framework and microporous materials are very important compounds due to their traditional applications in catalysis, separations, sorbents, and ion exchange, as well as their expected future use as hybrid composite materials in electro-optical and sensing applications.[1,2] Recently a number of metal carboxylates with open-framework network structure have been reported.[3] In the chemistry of metal phosphonates, the use of bifunctional or multifunctional anionic units, such as diphosphonates, aminophosphonates or phosphonocarboxylates has led to a number of new materials with microporous or open-framework structures.[4−7] Recently we have also reported a microporous Cd^{II} complex with *N*,*N*′-bis(phosphonomethyl)-1,10-diaza-18-crown ether.[8] Several porous Zr^{IV} complexes with aza-crown ether functionalised phosphonic acids have been synthesized by using phosphoric acid as the spacer group.[9] Direct use of two types of ligands in the preparation, such as a phosphonic acid and a carboxylic acid, has been found to be a useful method to build hybrid open frameworks, though such reports are still rare.[2,10] A 3D open-framework tin(II) phosphonopropionate oxalate and a layered tin(II) methylphosphonate oxalate have been reported by the Cheetham group,[10] and a microporous zinc(II) complex of phosphonopropionic acid and 1,3,5-benzenetricarboxylic acid (H_3BTC) was isolated; however, the tricarboxylate moiety remains noncoordinated and is also severely disordered.[2] We have synthesized a new amino diphosphonic acid, [3-pyridyl-$CH_2N(CH_2PO_3H_2)_2$] (H_4L^1) and a new amino triphosphonic acid, 1-[{$(H_2O_3PCH2)_2NCH_2CH_2$-}-piperazine-4-$CH_2PO_3H_2$] (H_6L^2) (Scheme 1). These two ligands are different from the aminodiphosphonic and -triphosphonic acids, which we had used previously: H_4L^1 contains an additional nitrogen atom for coordination; H_6L^2 has three methylenephosphonate groups attached to two different amine groups which are far apart, whereas the aminotriphosphonate ligand such as nitrilotris(methylenephosphonic acid) has three phosphonate groups attached to the same amine group.[11,12] Thus these new types of ligands are expected to be more likely to form novel hybrid materials with porous 3D network architectures. Hydrothermal reactions of the above two ligands with lead(II) acetate and 1,3,5-benzenetricarboxylic acid afforded two novel porous

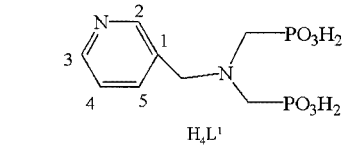

H_4L^1

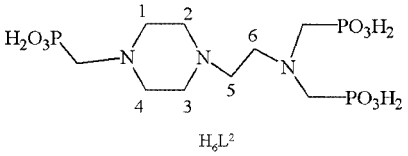

H_6L^2

Scheme 1. The structures of H_4L^1 and H_6L^2

[a] State Key Laboratory of Structural Chemistry,
Fujian Institute of Research on the Structure of Matter,
Chinese Academy of Sciences,
Fuzhou 350002, P. R. China
Fax: (internat.) +86-591-3714946
E-mail: mjg@ms.fjirsm.ac.cn
[b] Department of Chemistry, Texas A&M University,
P. O. Box 30012, College Station,
Texas 77843-3255

  DOI: 10.1002/ejic.200300417

lead(II) carboxylate-phosphonates in which both types of ligands act as multidentate metal linkers, $[Pb_4(BTC)(HBTC)(HL^1)]\cdot 3H_2O$ (**1**) and $[Pb_6(BTC)_2(HBTC)(H_2L^2)]\cdot 4.5H_2O$ (**2**). Herein we report their syntheses, characterizations and crystal structures.

Results and Discussion

The crystal structure of **1** features a 3D porous network of lead(II) tricarboxylate and a 1D double chain of lead diphosphonate, which are interconnected by sharing some Pb^{II} ions. There are four Pb^{II} atoms, one fully deprotonated tricarboxylate anion (BTC, O7 to O12), one 1H-protonated tricarboxylate (HBTC, O1 to O6), one 1H-protonated diphosphonate (HL^1) anion, and three lattice water molecules in an asymmetric unit of **1**. The coordination geometries around the lead(II) ions are shown in Figure 1. Pb1 is four-coordinated by three phosphonate oxygen atoms from three HL^1 ligands and one carboxylate oxygen atom from a BTC anion, whereas Pb3 is four-coordinated by two phosphonate and two carboxylate oxygen atoms from two HL^1 and two HBTC ligands, respectively. Their coordination geometry can be described as a ψ-square pyramidal PbO_4 in which the lone pair occupies the fifth coordination site. Pb2 is solely coordinated by diphosphonate ligands; it is four-coordinated by a tridentate chelating HL^1 ligand (ligating through two O and one N atoms) and a phosphonate oxygen atom from another HL^1 anion with a ψ-square pyramidal PbO_3N, similar to those of Pb1 and Pb3.

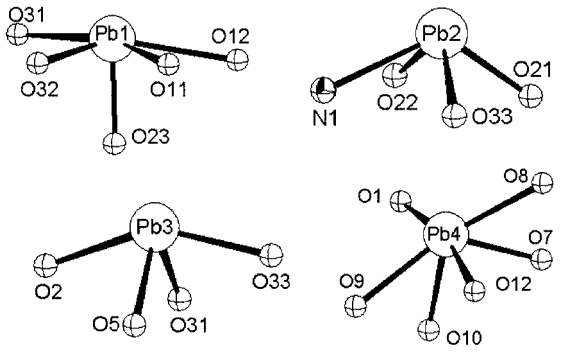

Figure 1. Coordination geometries of the lead(II) ions in **1**

This kind of coordination geometry has been reported in tin(II) phosphonopropionate oxalate and lead phosphonopropionate.[6,10] Pb4 is solely coordinated by tricarboxylate ligands; it is six-coordinated by two bidentate chelating carboxylate groups and two unidentate carboxylate groups from four carboxylate ligands. The coordination geometry around Pb4 can be described as a severely distorted ψ-pentagonal bipyramidal PbO_6 in which the seventh coordination site is occupied by the lone pair of the Pb^{II} ion. The coordination modes of the diphosphonate and BTC ligands are shown in Figure 2.

Each diphosphonate anion chelates with one Pb^{II} ion and bridges six other Pb^{II} ions. Atoms O31 and O33 are bidentate, whereas the remaining phosphonate oxygen atoms are unidentate. The Pb−O distances range from 2.30(2) Å to 2.71(2) Å, similar to those reported for other lead(II) phosphonates and lead(II) carboxylates.[6,7,12,13] The $[BTC]^{3-}$ anion is hexadentate and chelates with two lead(II) ions and also bridges two other lead(II) ions, whereas the $[HBTC]^{2-}$ anion acts as a tridentate ligand and bridges three Pb^{II} ions through two carboxylate groups. The third carboxylate group remains noncoordinated and protonated, as indicated by the longer C18−O4 distance. Based on charge balance, P−O distances, and its coordination mode, the diphosphonate anion should have a charge of −3; hence the pyridyl N atom must be also protonated.

It was noticed that diphosphonate or BTC ligands in $[Pb_4(BTC)(HBTC)(HL^1)]\cdot 3H_2O$ alone can form a coordination polymer with the lead(II) ions. Each pair of $[Pb(HL^1)]$ chelating units is bridged by a pair of phosphonate groups to form a dimer. Such dimers are further interconnected by Pb1 and Pb3 atoms, resulting in the formation of a $[Pb_3(HL^1)]^{3-}$ anionic double chain along the *a*-axis (Figure 3a). The interconnection of lead(II) ions (Pb1, Pb3 and Pb4) by bridging BTC and HBTC ligands results in a $[Pb_3(BTC)(HBTC)]^+$ cation whose structure is also a 3D porous network with two types of tunnels (Figure 3b).

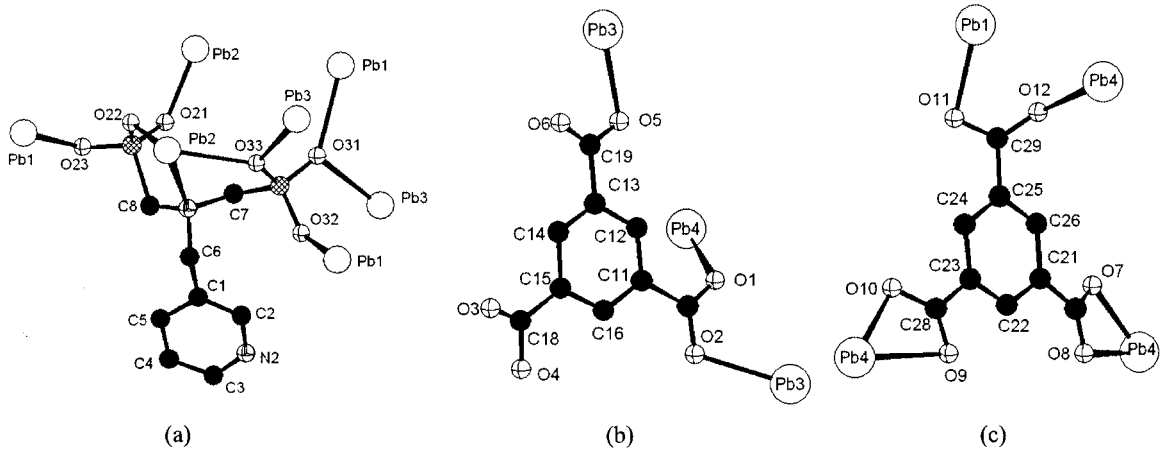

Figure 2. Coordination modes for the diphosphonate and BTC ligands in **1**: (a) HL^1; (b) $[BTC]^{3-}$; (c) $[HBTC]^{2-}$

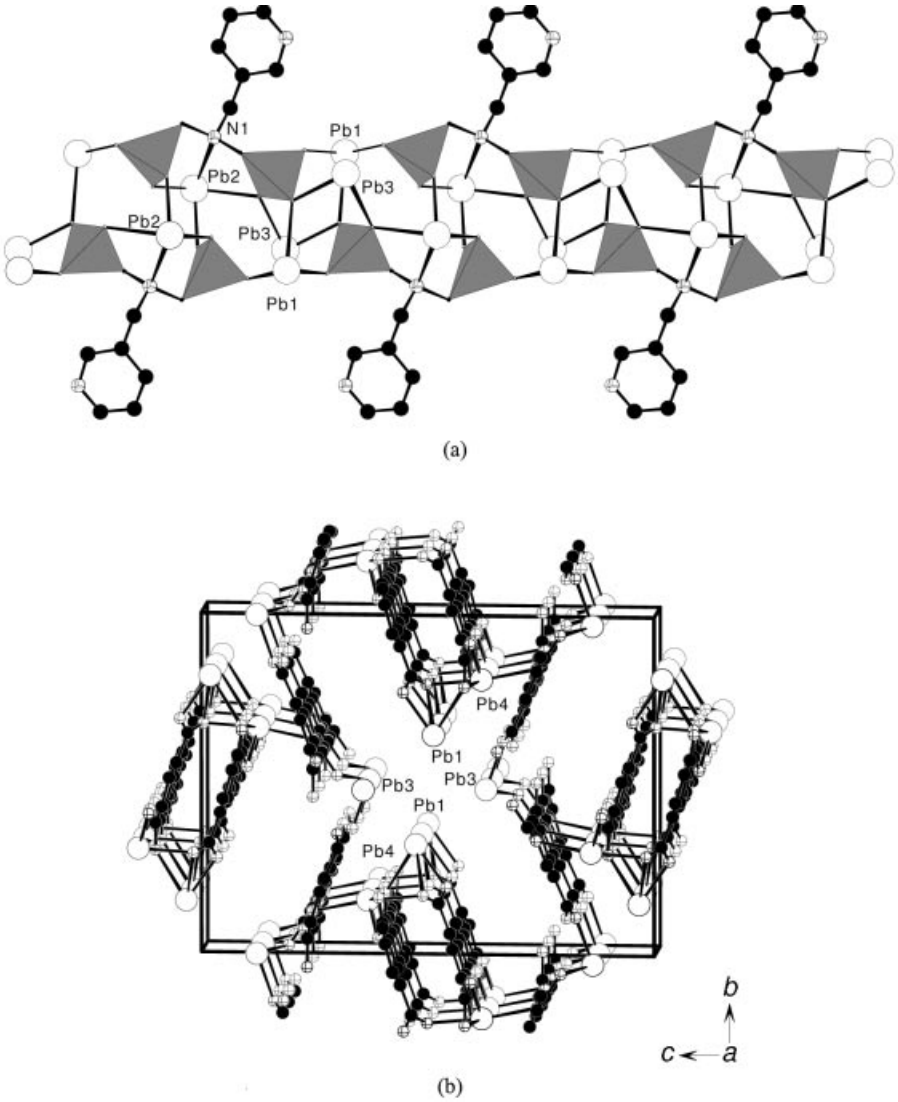

Figure 3. The 1D double chain of lead(II) diphosphonate along the *a*-axis in **1**(a) and the porous 3D network of lead(II) 1,3,5-benzenetricarboxylate in **1** (b); the C-PO_3 tetrahedra are shaded in gray, Pb, N, O and C atoms are represented by open, octanded, crossed and black circles, respectively

The smaller cavity is ca 8.0 $Å^2$ wide and is formed by 16-member rings, each of which is composed of two Pb1 atoms and two BTC ligands. The larger cavity is formed by 54-membered rings, each of which is formed by 8 Pb atoms and 8 BTC ligands. The size of the larger channel is estimated to be about 1/4 of the cell volume. This kind of arrangement is similar to that reported in $Pb_3(BTC)_2{\cdot}H_2O$.[13] These two types of coordination polymeric anions and cations are interconnected through atoms Pb1 and Pb3, resulting in the formation of a new porous network (Figure 4). Such linkage cuts the large cavity of $[Pb_3(BTC)(HBTC)]^+$ in half, thus greatly reducing the cavity size. The pyridine and noncoordinated carboxylate groups are directed towards the micropores. The lattice water molecules also occupy the cavity of the pores, forming hydrogen bonds with noncoordinated carboxylate oxygen atoms, which further increase the stability of the structure (Table 1).

The structure of **2** contains six Pb^{II} ions, two $[BTC]^{3-}$ anions, one $[HBTC]^{2-}$ anion and a 2H-protonated triphosphonate ligand (H_2L^2) in an asymmetric unit. Both Pb1 and Pb3 are five-coordinated by four carboxylate oxygen atoms from two BTC and one HBTC ligands as well as a phosphonate oxygen atom (Figure 5).

Pb2 is six-coordinated by four carboxylate oxygen atoms from one HBTC and two BTC ligands, and two phosphoate oxygen atoms from a bidentate chelating phosphonate group. Pb4 is five-coordinated by three carboxylate oxygen atoms from one BTC and one HBTC anions, and two phosphonate oxygen atoms from two phosphonate groups. Pb5 is four-coordinated by a chelating carboxylate group of a HBTC ligand and two phosphonate oxygen atoms from two L^2 ligands. Pb6 is five-coordinated by a tridentate chelating L^2 ligand (through N2, O41 and O33), a phosphonate oxygen from a neighboring L^2 ligand and a carboxylate oxygen atom of a BTC anion. The four-, five- and six-coordinate

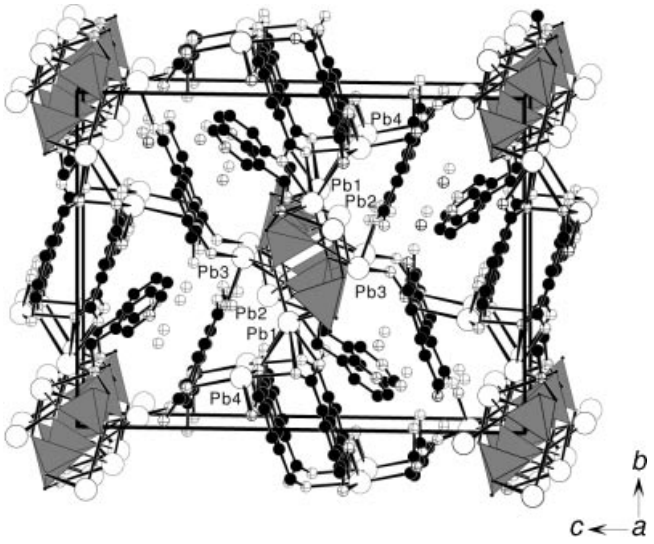

Figure 4. View of the structure of **1** down the *a*-axis; the C-PO_3 tetrahedra are shaded in gray, Pb, N, O and C atoms are represented by open, octanded, crossed and black circles, respectively

lead(II) ions have quite different coordination geometries: ψ-square pyramidal PbO_4, ψ-octahedral PbO_5 (or PbO_4N) and ψ-pentagonal bipyramidal PbO_6 (the lone pairs occupying the fifth, sixth and seventh coordination sites), which are similar to those in compound **1**. The Pb−O distances range from 2.27(1) to 2.75(1) Å and the P−N distance is 2.67(2) Å, which are similar to those in **1** and other lead(II) phosphonates.[6,7,12]

The aminotriphosphonate ligand adopts an interesting coordination mode (Figure 6). The phosphonate group containing P2 forms a chelate with the Pb2 atom (through O21 and O23) and bridges the Pb1 and the Pb3 atom. The O22 atom remains noncoordinated and forms a hydrogen bond with the noncoordinated carboxylate oxygen atom (O10; Table 2). The $N(CH_2PO_3)_2$ moiety of the L^2 ligand is octadentate; it chelates with Pb6 as a tridentate ligand (through N2, O33 and O41) and also bridges five other Pb^{II} ions (two Pb5, two Pb4 and one Pb6 atom). Three phosphonate oxygen atoms (O21, O23 and O41) are bidentate metal linkers. The two nitrogen atoms of the piperazine ring are 1H-

Table 1. Selected bond lengths (Å) and angles (°) for complex **1**

Selected Bonds[a]			
Pb1−O32	2.300(15)	Pb1−O(23)#1	2.341(15)
Pb1−O11	2.460(17)	Pb1−O(31)#2	2.684(15)
Pb2−O(21)#3	2.275(15)	Pb2−O22	2.320(15)
Pb2−O33	2.570(15)	Pb2−N1	2.711(17)
Pb3−O5	2.420(16)	Pb3−O31	2.428(13)
Pb3−O(33)#2	2.575(15)	Pb3−O(2)#4	2.586(18)
Pb4−O(7)#5	2.32(2)	Pb4−O(10)#6	2.36(2)
Pb4−O(12)#2	2.59(2)	Pb4−O(8)#5	2.62(2)
Pb4−O(9)#6	2.70(3)	Pb4−O1	2.70(3)
	Hydrogen bonds		
O4···O(2w)#7	2.86(4)	O4···O(6)#8	2.67(3)
O(1w)···O(2w)	2.41(5)	O(2w)···O(3w)	2.77(4)
O3···O(1w)#1	2.73(5)		
O32−Pb1−O(23)#1	79.4(5)	O32−Pb1−O11	77.1(5)
O(23)#1−Pb1−O11	78.7(6)	O32−Pb1−O(31)#2	80.7(5)
O(23)#1−Pb1−O(31)#2	90.8(5)	O11−Pb1−O(31)#2	156.8(5)
O(21)#3−Pb2−O22	83.2(6)	O(21)#3−Pb2−O33	76.5(5)
O22−Pb2−O33	115.7(5)	O(21)#3−Pb2−N1	120.8(5)
O22−Pb2−N1	71.5(5)	O33−Pb2−N1	68.9(5)
O5−Pb3−O31	83.7(5)	O5−Pb3−O(33)#2	82.9(6)
O31−Pb3−O(33)#2	79.0(5)	O5−Pb3−O(2)#4	76.0(6)
O31−Pb3−O(2)#4	74.5(6)	O(33)#2−Pb3−O(2)#4	147.6(5)
O(7)#5−Pb4−O(10)#6	81.7(9)	O(7)#5−Pb4−O(12)#2	80.3(8)
O(10)#6−Pb4−O(12)#2	81.5(7)	O(7)#5−Pb4−O(8)#5	51.7(8)
O(10)#6−Pb4−O(8)#5	130.9(7)	O(12)#2−Pb4−O(8)#5	76.9(6)
O(7)#5−Pb4−O(9)#6	128.5(8)	O(10)#6−Pb4−O(9)#6	51.3(8)
O(12)#2−Pb4−O(9)#6	73.8(6)	O(8)#5−Pb4−O(9)#6	149.8(7)
O(7)#5−Pb4−O1	102.7(8)	O(10)#6−Pb4−O1	85.0(8)
O(12)#2−Pb4−O1	165.6(7)	O(8)#5−Pb4−O1	116.2(7)
O(9)#6−Pb4−O1	93.8(7)		

[a] Symmetry transformations used to generate equivalent atoms: #1 $x-1, y, z$; #2 $-x, -y+1, -z+1$; #3 $-x+1, -y+1, -z+1$; #4 $-x+1/2, y+1/2, -z+3/2$; #5 $x+1, y-1, z$; #6 $x, y-1, z$; #7 $1/2-x, -1/2+y, 3/2-z$; #8 $-1/2-x, -1/2+y, 3/2-z$.

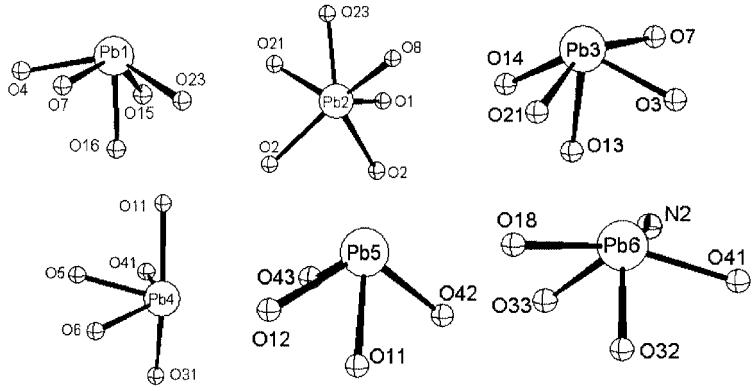

Figure 5. The coordination geometries around the lead(II) ions in **2**

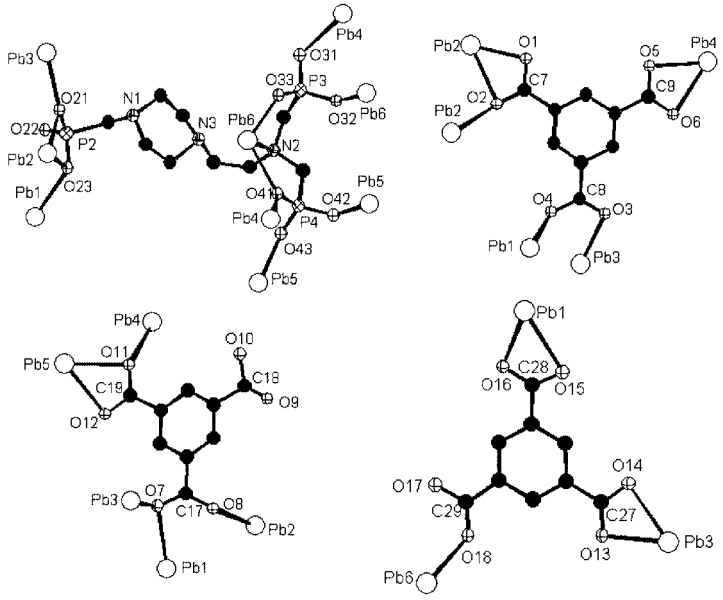

Figure 6. The coordination modes of L^2 and 1,3,5-benzenetricarboxylate ligands in **2**

protonated and remain noncoordinated. The three 1,3,5-benzyltricarboxylate ligands in **2** adopt three different types of coordination modes (Figure 6).

The BTC ligand containing O1 to O6 is heptadentate and bridges five Pb^{II} ions. The carboxylate group CO1O2 forms three bonds, a chelate to one Pb2 atom and a bridge between the two Pb2 atoms, the one containing CO3O4 bridges Pb1 and Pb3 (two-coordinated), whereas the one composed of CO5O6 forms a chelate with Pb4 (two-coordinated). The second tricarboxylate ligand containing O7 to O12 is hexadentate. One carboxylate group CO7O8 bridges three Pb^{II} ions (three bonds to Pb1, Pb2, and Pb3), the second carboxylate group CO11O12 forms three bonds (a chelate with Pb5 and a bridge between Pb4 and Pb5). The third carboxylate group CO9O10 is noncoordinated, and the O10 atom remains protonated as indicated by its longer C−O distance. Thus it is a $[HBTC]^{2-}$ anion. The third BTC ligand (O13 to O18) is pentadentate two carboxylate groups (CO13O14 and CO15O16) are bidentate chelating whereas the third (CO17O18) is unidentate. The atoms O2, O7 and O11 are bidentate metal linkers.

The interconnection of Pb4, Pb5 and Pb6 atoms by the $N(CH_2PO_3)_2$ moieties of L^2 ligands resulted in a 1D double chain along the *a*-axis (Figure 7a). Pb1, Pb2 and Pb3 atoms form a <002> corrugated carboxylate−phosphonate hybrid layer with carboxylate ligands and the phosphonate groups containing P2 atoms (Figure 7b), resulting in the formation of several types of rings. One is the four-membered ring formed by Pb1, O4, Pb3 and O7 atoms. The second type is the six-membered ring formed by Pb1, O23, Pb2, O8, C17 and O7 atoms. The third one is the 12-membered ring composed of four Pb^{II} ions (two Pb2 and two Pb3), two bridging carboxylate groups (two CO7O8) and two bidentate O14 atoms.

The above 1D lead(II) phosphonate double chains and <002> hybrid layers are cross-linked through the organic

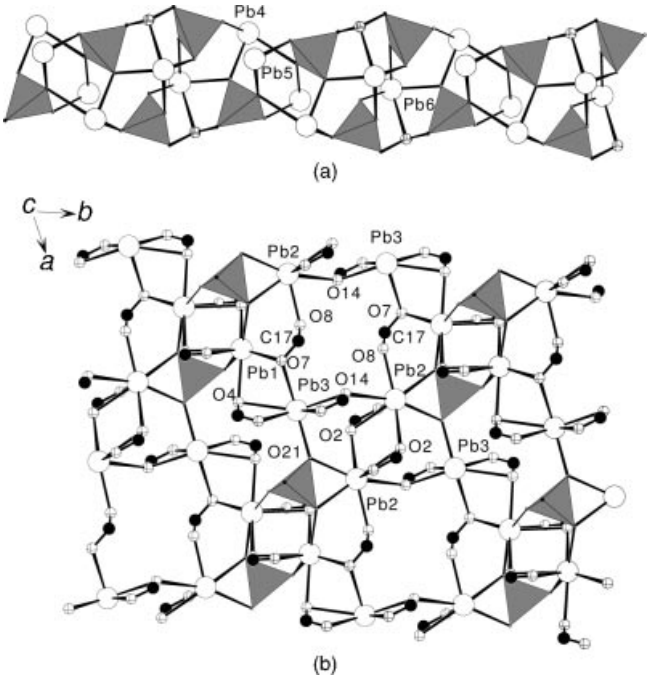

Figure 7. The 1D double chain of lead(II) diphosphonate along the *a*-axis (a) and a <002> lead(II) carboxylate−phosphonate hybrid 2D layer (b) in complex **2**; the C-PO_3 tetrahedra are shaded in gray, Pb, N, O and C atoms are represented by open, octanded, crossed and black circles, respectively.

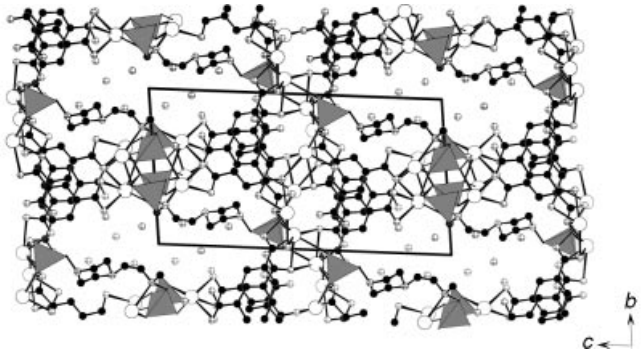

Figure 8. View of the porous 3D network of **2** down the *a*-axis; the C-PO_3 tetrahedra are shaded in gray, Pb, N, O and C atoms are represented by open, octanded, crossed and black circles, respectively

groups of HBTC, BTC and H_2L^2 ligands to form a porous 3D network (Figure 8). The size of the pore is estimated to be 4.0 × 16.0 Å^2. The lattice water molecules are located at these micropores and are involved in hydrogen bonding (Table 2).

The XRD powder patterns for compounds **1** and **2** were collected on a Philips X'Pert-MPD diffractometer using graphite-monochromated Cu-K_α radiation in the angular range $2\theta = 5-70°$. Their powder patterns match with the ones calculated from their single crystal structure data, thus both compounds exist as a single phase.

IR spectra of compounds **1** and **2** show the asymmetric and symmetric vibrations of the carboxyl group at 1543 and 1431 cm^{-1} for **1**, and 1531 and 1433 cm^{-1} for **2**, respectively. The vibrations of the phosphonic groups are in the region 900−1100 cm^{-1}.[7] The broad bands at 3392 cm^{-1} (**1**) and 3396 cm^{-1} (**2**) indicate the presence of the water molecules in both compounds.

The TGA diagram of **1** shows three main steps of the weight losses. The first step is loss of three lattice water molecules, which started at 62 °C and was completed at 165 °C, the observed weight loss of 3.2% is in good agreement with the calculated value (3.4%). The second step covering a temperature range of 320 °C to 633 °C corresponds to the burning of BTC and diphosphonate ligands. The third step overlapped with the second one, corresponding to further decomposition of organic groups. The final products are $Pb_2P_2O_7$ and PbO in a 1:2 molar ratio. The total weight loss of 33.0% is close to the calculated value (35%). The TGA curves of **2** also exhibit three steps of weight loss. The first step is the release of the lattice water molecules, which started at 33°C and was completed at 155°C; the observed weight loss of 3.46% matches with the theoretical one (3.44%). The second and third steps are overlapped, starting at 340 °C and continued up to 1000 °C, during which two processes occurred, firstly, the decomposition of the BTC ligands, and secondly, the burning of the triphosphonate ligand. The final products are assumed to be $Pb_2P_2O_7$ and PbO in a molar ratio of 1:2. The total weight loss of 31.8% is close to the calculated one (34.1%).

Conclusion

In summary, the hydrothermal reactions of lead(II) acetate with an aminodiphosphonic or an aminotriphosphonic acid and 1,3,5-benzenetricarboxylic acid resulted in two novel porous lead(II) carboxylate−phosphonate hybrids in which both ligands act as multidentate metal linkers. The 1,3,5-benzenetricarboxylate ligand may also act as a pillar agent or an intercalated species between two metal phosphonate layers. Thus we believe that a wide range of new open frameworks and microporous materials can be developed by using this technique.

Experimental Section

Materials and Methods: All chemicals were obtained from commercial sources and used without further purification. Elemental analyses were performed on a Vario EL III elemental analyzer. Thermogravimetric analyses were carried out with a TGA/SBTA851 unit at a heating rate of 15 °C/min under an oxygen atmosphere. IR spectra were recorded on a Magna 750 FT-IR spectrometer photometer as KBr pellets in the range 4000−400 cm^{-1}. ^{1}H and ^{31}P NMR spectra were recorded on a Varian Unity 500 NMR in D_2O. H_3PO_4 was used as the ^{31}P standard reference. The XRD powder patterns were collected on a Philips X'Pert-MPD diffractometer using graphite-monochromated Cu-K_α radiation in the angular range $2\theta = 5-70°$ with a step size of 0.02° and a counting time of 3 s per step.

Preparation of H_4L^1 and H_6L^2: H_4L^1 was prepared by a Mannich type reaction according to the procedures previously described.[11] 3-(Aminomethyl)pyridine (100 mmol, 12.6 mL) was mixed with

Table 2. Selected bond lengths (Å) and angles (°) for complex **2**.

Selected bonds[a]			
Pb1−O7	2.545(12)	Pb1−O(4)#1	2.569(11)
Pb1−O(16)#1	2.569(12)	Pb1−O23	2.587(11)
Pb1−O(15)#1	2.753(13)	Pb2−O1	2.437(13)
Pb2−O8	2.520(11)	Pb2−O21	2.573(11)
Pb2−O23	2.596(12)	Pb2−O2	2.679(12)
Pb2−O(2)#2	2.704(11)	Pb3−O21	2.400(11)
Pb3−O(3)#3	2.430(12)	Pb3−O13	2.506(13)
Pb3−O14	2.571(13)	Pb3−O(7)#4	2.647(12)
Pb4−O41	2.445(11)	Pb4−O(31)#5	2.472(15)
Pb4−O5	2.530(13)	Pb4−O6	2.598(14)
Pb4−O11	2.751(13)	Pb5−O(42)#6	2.331(14)
Pb5−O43	2.355(13)	Pb5−O11	2.615(14)
Pb5−O12	2.646(15)	Pb6−O33	2.274(13)
Pb6−O(32)#5	2.438(14)	Pb6−O41	2.510(11)
Pb6−O18	2.663(13)	Pb6−N2	2.671(16)
Hydrogen bonds			
O10···O(22)#7	2.587(19)	O(1w)···O(3w)#1	2.80(5)
O(1w)···O(6w)	2.57(9)	O(2w)···O(7w)	2.51(8)
O(3w)···O(4w)	2.51(6)	O(4w)···O(7w)#6	2.44(8)
O7−Pb1−O(4)#1	74.5(4)	O7−Pb1−O(16)#1	89.7(4)
O(4)#1−Pb1−O(16)#1	76.6(4)	O7−Pb1−O23	76.2(4)
O(4)#1−Pb1−O23	139.3(4)	O(16)#1−Pb1−O23	75.5(4)
O7−Pb1−O(15)#1	138.1(4)	O(4)#1−Pb1−O(15)#1	84.7(4)
O(16)#1−Pb1−O(15)#1	49.7(4)	O23−Pb1−O(15)#1	99.0(4)
O1−Pb2−O8	93.3(4)	O1−Pb2−O21	86.5(4)
O8−Pb2−O21	124.2(4)	O1−Pb2−O23	88.5(4)
O8−Pb2−O23	67.4(4)	O21−Pb2−O23	56.8(3)
O1−Pb2−O2	50.4(4)	O8−Pb2−O2	109.8(4)
O21−Pb2−O2	112.1(4)	O23−Pb2−O2	138.9(4)
O1−Pb2−O(2)#2	109.8(4)	O8−Pb2−O(2)#2	151.7(4)
O21−Pb2−O(2)#2	74.9(4)	O23−Pb2−O(2)#2	127.2(4)
O2−Pb2−O(2)#2	75.7(4)	O21−Pb3−O(3)#3	83.5(4)
O21−Pb3−O13	74.1(4)	O(3)#3−Pb3−O13	77.6(4)
O21−Pb3−O14	91.2(4)	O(3)#3−Pb3−O(14)	127.6(4)
O13−Pb3−O14	51.2(4)	O21−Pb3−O(7)#4	150.0(4)
O(3)#3−Pb3−O(7)#4	76.5(4)	O13−Pb3−O(7)#4	79.9(4)
O14−Pb3−O(7)#4	83.8(4)	O41−Pb4−O(31)#5	81.4(5)
O41−Pb4−O5	76.4(4)	O(31)#5−Pb4−O5	100.8(4)
O41−Pb4−O6	120.9(4)	O(31)#5−Pb4−O6	83.2(5)
O5−Pb4−O6	51.3(4)	O41−Pb4−O11	81.6(5)
O(31)#5−Pb4−O11	162.9(5)	O5−Pb4−O11	74.4(4)
O6−Pb4−O11	105.1(5)	O(42)#6−Pb5−O43	81.8(4)
O(42)#6−Pb5−O11	71.6(4)	O43−Pb5−O11	95.9(5)
O(42)#6−Pb5−O12	118.4(5)	O43−Pb5−O12	86.5(5)
O11−Pb5−O12	49.8(5)	O33−Pb6−O(32)#5	79.4(5)
O33−Pb6−O41	116.0(4)	O(32)#5−Pb6−O41	79.9(4)
O33−Pb6−O18	73.0(4)	O(32)#5−Pb6−O18	74.5(4)
O41−Pb6−O18	150.8(4)	O33−Pb6−N2	73.4(5)
O(32)#5−Pb6−N2	127.0(4)	O41−Pb6−N2	72.9(4)
O18−Pb6−N2	134.7(4)		

[a] Symmetry transformations used to generate equivalent atoms: #1 $x-1, y+1, z$; #2 $-x+1, -y+1, -z+1$; #3 $x, y+1, z$; #4 $x+1, y, z$, #5 $-x+1, -y+1, -z$; #6 $-x, -y+1, -z$; #7 $x, -1+y, z$.

37% hydrochloric acid (16.0 mL), deionized water (20 mL) and phosphorous acid (400 mmol, 32.8 g). The mixture was allowed to reflux at 120 °C for 1 h, then paraformaldehyde (300 mmol, 9 g) was added in small portions over a period of 1 h, and the mixture was refluxed for an additional hour. Removal of the solvents afforded 26.4 g of a white powder of H_4L^1 (yield 89.2%). Its purity was confirmed by NMR measurements and elemental analysis. ^{31}P NMR spectrocopy shows a single peak at $\delta = 7.97$ ppm. ^1H NMR: $\delta = 3.51$ ppm (N-CH_2-PO_3, d, 4 H, $J_{H,P} = 12.5$ Hz), 5.02 ppm (pyridine-CH_2-N, s, 2 H), 8.21 ppm [C(4)H, 1 H, t], 8.91 ppm [C(5)H, 1 H, d, $J_{H,H} = 5.5$ Hz], 8.93 ppm [C(3)H, d, $J_{H,H} = 8.5$ Hz], 9.15 ppm [C(2)H, 1 H, s], refer to Scheme 1 for the labeling of the carbon atoms. $C_8H_{14}N_2O_6P_2$ (296.2): calcd. C 32.45, H 4.76, N 9.46; found C 32.53, H 4.98, N 9.23. IR (KBr): $\tilde{\nu} = 3428$ cm^{-1} s, 3317 w, 3093 m, 3002 w, 2162 m, 2009 w, 1678 m, 1574 w, 1518 s, 1431 m, 1296 m, 1225 m, 1173 s, 1124 s, 1074 s, 1049 s, 1003 vs,

Table 3. Crystal data and structure refinement for complexes **1** and **2**

Compound	**1**	**2**
Formula	$C_{26}H_{24}N_2O_{21}P_2Pb_4$	$C_{36}H_{39}N_3O_{31.5}P_3Pb_6$
M_r	1591.17	2353.75
Space group	$P2_1/n$	$P\bar{1}$
a (Å)	10.1516(4)	10.3370(2)
b (Å)	15.8101(6)	12.5019(3)
c (Å)	21.7442(9)	21.8254(3)
α (°)	90.0	83.473(1)
β (°)	102.252(2)	86.896(1)
γ (°)	90.0	68.040(1)
V (Å^3)	3410.4(2)	2598.74(9)
Z	4	2
$D_{calcd.}$ (g.cm^{-3})	3.099	3.008
μ (mm^{-1})	19.875	19.560
Total reflections	11442	13226
Unique reflections	5946	8937
No. of parameters refined	497	653
GooF on F^2	1.054	1.106
$R1$, $wR2$ [$I > 2\sigma(I)$][a]	0.0716/0.1896	0.055/0.1042
$R1$, $wR2$ (all data)	0.0901/0.2070	0.0941/0.1231

[a] $R1 = \Sigma(F_o - F_c)/\Sigma F_o$; $wR2 = \{\Sigma w[(F_o)^2 - (F_c)^2]^2/\Sigma w[(F_o)^2]^2\}^{1/2}$.

951 vs, 920 s, 833 m, 816 m, 802 m, 760 m, 717 m, 692 m, 636 m, 627 m, 553 m, 476 s.

H_6L^2 was prepared in a yield of 86.8% by a Mannich type reaction of 1-(2-aminomethyl)piperazine (100 mmol, 13.2 mL), 37% hydrochloric acid (30 mmol), deionized water (32.0 mL), phosphorous acid (700 mmol, 57.4 g) and paraformaldehyde (500 mmol, 15 g) in a similar method to that of H_4L^1. ^{31}P NMR spectroscopy shows two peaks at δ = 7.18 ppm (for piperazine-CH_2-PO_3H_2) and 11.00 ppm [for $N(CH_2PO_3H_2)_2$], respectively. ^1H NMR: δ = 3.50 ppm (N-CH_2-PO_3, d, 6 H, $J_{H,P}$ = 12.5 Hz), 3.66 ppm [C(5)H_2 and C(6)H_2, t, 4 H], 3.86 ppm [C(1)H_2-C(4)H_2, t, 8 H]. $C_9H_{24}N_3O_{12}P_3$ (459.2): calcd. C 23.54, H 5.27, N 9.15; found. C 23.62, H 5.60, N 9.06. IR (KBr): $\tilde{\nu}$ = 3498 cm^{-1} m, 3392 m, 3342 m, 3016 m, 3016 m, 1662 w, 1629 w, 1521 w, 1458 m, 1433 m, 1383 w, 1271 m, 1174 s, 1119 vs, 1057 m, 1024 m, 985 s, 947 s, 923 m, 769 m, 548 s, 455 m.

Synthesis of $[Pb_4(BTC)(HBTC)(HL^1)]\cdot 3H_2O$ (1) and $[Pb_6(BTC)_2(HBTC)(H_2L^2)]\cdot 4.5H_2O$ (2): $[Pb_4(BTC)(HBTC)(HL^1)]\cdot 3H_2O$ (**1**) was prepared by hydrothermal reaction of lead(II) acetate trihydrate (0.75 mmol, 0.29 g), H_4L^1 (0.25 mmol, 0.08 g) and H_3BTC (0.5 mmol, 0.10 g) in a 3:1:2 molar ratio in 10.0 mL of deionized water at 150 °C for 3 days. Colorless crystals of **1** were recovered in 45.8% yield (based on Pb). $C_{26}H_{22}N_2O_{21}P_2Pb_4$ (1591.17): calcd C 19.65, H 1.40, N 1.76; found C 19.53, H 1.27, N 1.72. IR (KBr): $\tilde{\nu}$ = 3392 cm^{-1} m, 1697 m, 1610 s, 1543 s, 1527 s, 1431 s, 1354 vs, 1261 m, 1190 m, 1095 m, 1061 s, 989 w, 939 w, 843 w, 816 w, 760 w, 721 s, 683 w, 586 m, 569 w, 515 m. $[Pb_6(BTC)_2(HBTC)(H_2L^2)]\cdot 4.5H_2O$ (**2**) was prepared by hydrothermal reactions of lead(II) acetate trihydrate (0.75 mmol, 0.29 g) H_6L^2 (0.25 mmol, 0.11 g) and H_3BTC (0.5 mmol, 0.10 g) in a 3:1:2 molar ratio in 10.0 mL of deionized water at 180 °C for 3 days. Colorless crystals of **2** were recovered in 46.4% yield (based on Pb). $C_{36}H_{40}N_3O_{32}P_3Pb_6$ (2353.75): calcd. C 18.30, H 1.71, N 1.78; found C 18.43, H 1.98, N 1.64. IR (KBr): $\tilde{\nu}$ = 3396 cm^{-1} m, 1651 w, 1610 m, 1531 s, 1433 s, 1361 vs, 1311 m, 1219 w, 1095 s, 1039 s, 966 s, 817 w, 802 w, 758 m, 721 s, 694 w, 572 m, 555 w, 509 w, 482 w.

Crystal Structure Determination: Single crystals of **1** and **2** were mounted on a Siemens Smart CCD diffractometer equipped with a graphite-monochromated Mo-K_α radiation (λ = 0.71073 Å). Intensity data were collected by the narrow frame method at 293 K. The data sets were corrected for Lorentz and polarization as well as for absorption by ψ scan technique. Both structures were solved by direct methods and refined by full-matrix least-squares fitting on F^2 by SHELX-97.[14] All non-hydrogen atoms, except for C7, C11, and O32 in **1**, and C6, C22, C25, C31, C32, C33, C34, C35 and O(7 W) in **2,** were refined with anisotropic thermal parameters. The carbon atoms of the piperazine ring in **2** have large thermal parameters and were refined with a rigid model. Lattice water molecules [O(3 W) to O(7 W)] also have large thermal parameters, and each was assigned with an occupancy factor of 50%. Despite these problems, the refinement of **2** can still be considered satisfactory for such a complicated structure. The final difference Fourier maps showed featureless residual peaks of 2.88 [for, **1**, 1.15 Å from the Pb4 atom] and 1.78 e·Å^{-3} [for **2**, 0.84 from the Pb6 atom], respectively. All hydrogen atoms were located at geometrically calculated positions. The hydrogen atoms for the water molecules were not included in the refinement. Crystallographic data and structural refinement are summarized in Table 3. Important bond lengths and angles are listed in Table 1 for complex **1** and Table 2 for complex **2**. CCDC-209007 and -209008 contain the supplementary crystallographic data for this paper. These data can be obtained free of charge at www.ccdc.cam.ac.uk/conts/retrieving.html [or from the Cambridge Crystallographic Data Centre, 12 Union Road, Cambridge CB2 1EZ, UK; Fax: (internat.) + 44-1223-336-033; E-mail: deposit@ccdc.cam.ac.uk].

Acknowledgments

This work was supported by the Innovative Project, "The Introduction of Overseas Elitists Program by the Chinese Academy of Sciences and the Scientific Research Foundation for the Returned Overseas Chinese Scholars, State Education Ministry."

[1] A. K. Cheetham, G. Ferey, T. Loiseau, *Angew. Chem. Int. Ed.* **1999**, *38*, 3268−3292.

[2] J. Zhu, X. Bu, P. Feng, G. D. Stucky, *J. Am. Chem. Soc.* **2000**, *122*, 11563−11564.
[3] N. L. Rosi, M. Eddaoudi, J. Kim, M. O'Keeffe, O. M. Yaghi, *Angew. Chem. Int. Ed.* **2001**, *41*, 284−310; M. Eddaoudi, J. Kim, M. O'Keeffe, O. M. Yaghi, *J. Am. Chem. Soc.* **2002**, *124*, 376−377; M. E. Braun, C. D. Steffek, J. Kim, P. G. Rasmussen, O. M. Yaghi, *Chem. Commun.* **2001**, 2532−2533.
[4] A. Distler, L. Lohse, S. C. Sevov, *J. Chem. Soc., Dalton Trans.* **1999**, 1805−1812; V. Soghomonian, Q. Chen, R. C. Haushalter, J. Zubieta, *Angew. Chem. Int. Ed. Engl.* **1995**, *34*, 223−226.
[5] S. Drumel, P. Janvier, D. Deniaud, B. Bujoli, *Chem. Commun.* **1995**, 1051−1052; U. Costantino, M. Nocchetti, R. Vivani, *J. Am. Chem. Soc.* **2002**, *124*, 8428−8434; S. O. H. Gutschke, D. J. Price, A. K. Powell, P. T. Wood, *Angew. Chem. Int. Ed.* **1999**, *38*, 1088−1090; E. Galdecka, Z. Galdecki, P. Gawryszewska, J. Legendziewicz, *New J. Chem.* **2000**, *24*, 387−391; L.-M. Zheng, P. Yin, X.-Q. Xin, *Inorg. Chem.* **2002**, *41*, 4084−4086.
[6] N. Stock, S. A. Frey, G. D. Stucky, A. K. Cheetham, *J. Chem. Soc., Dalton Trans.* **2000**, 4292−4296; S. Ayyappan, G. D. Delgado, A. K. Cheetham, G. Ferey, C. N. R. Rao, *J. Chem. Soc., Dalton Trans.* **1999**, 2905−2907; F. Fredoueil, M. Evain, D. Massiot, M. Bujoli-Doeuff, P. Janvier, A. Clearfield, B. Bujoli, *J. Chem. Soc., Dalton Trans.* **2002**, 1508−1512; S. Drumel, M. Bujolidoeuff, P. Janvier, B. Bujoli, *New J. Chem.* **1995**, *19*, 239−242.
[7] A. Distler, S. C. Sevov, *Chem. Commun.* **1998**, 959−960; S. J. Hartman, E. Todorov, C. Cruz, S. C. Sevov, *Chem. Commun.* **2000**, 1213−1214; J.-G. Mao, Z. Wang, A. Clearfield, *Inorg. Chem.* **2002**, *41*, 6106−6111; R. Vivani, U. Costantino, M. Nocchetti, *J. Mater. Chem.* **2002**, *12*, 3254−3260.
[8] J.-G. Mao, Z. Wang, A. Clearfield, *Inorg. Chem.* **2002**, *41*, 3713−3720.
[9] B. Zhang, A. Clearfield, *J. Am. Chem. Soc.* **1997**, *119*, 2751−2752; A. Clearfield, D. M. Poojary, B. Zhang, B. Zhao, A. Derecskei-Kovacs, *Chem. Mater.* **2000**, *12*, 2745−2752.
[10] N. Stock, G. D. Stucky, A. K. Cheetham, *Chem. Commun.* **2000**, 2277−2278; B. Adair, S. Natarajan, A. K. Cheetham, *J. Mater. Chem.* **1998**, *8*, 1477−1479.
[11] J.-G. Mao, Z. Wang, A. Clearfield, *Inorg. Chem.* **2002**, *41*, 2334−2340; J.-G. Mao, Z. Wang, A. Clearfield, *J. Chem. Soc., Dalton Trans.* **2002**, 4541−4546.
[12] A. Cabeza, M. A. G. Aranda, S. Bruque, A. Clearfield, *J. Mater. Chem.* **1999**, *9*, 571−578; J.-G. Mao, Z. Wang, A. Clearfield, *New J. Chem.* **2002**, *26*, 1010−1014; C. V. K. Sharma, A. Clearfield, A. Cabeza, M. A. G. Aranda, S. Bruque, *J. Am. Chem. Soc.* **2001**, *123*, 2885−2886; A. Cabeza, O. Y. Xiang, C. V. K. Sharma, M. A. G. Aranda, S. Bruque, A. Clearfield, *Inorg. Chem.* **2002**, *41*, 2325−2333.
[13] M. R. St J. Foreman, T. Gelbrich, M. B. Hursthouse, M. J. Plater, *Inorg. Chem. Commun.* **2000**, *3*, 234−238.
[14] G. M. Sheldrick, *SHELXTL*, *Crystallographic Software Package*, version 5.1, Bruker-AXS, Madison, WI, **1998**.

Received June 30, 2003
Early View Article
Published Online October 10, 2003

